The University of Akron
IdeaExchange@UAkron

Chemical and Biomolecular Engineering Faculty Research

Chemical and Biomolecular Engineering Department

7-1-2003

Nanoscale Oxidation of Zirconium Surfaces: Kinetics and Mechanisms

N. Farkas

G. Zhang

Edward A. Evans
University of Akron Main Campus, evanse@uakron.edu

R. D. Ramsier

J. A. Dagata

Please take a moment to share how this work helps you through this survey. Your feedback will be important as we plan further development of our repository.
Follow this and additional works at: http://ideaexchange.uakron.edu/chemengin_ideas

 Part of the Chemistry Commons

Recommended Citation
Farkas, N.; Zhang, G.; Evans, Edward A.; Ramsier, R. D.; and Dagata, J. A., "Nanoscale Oxidation of Zirconium Surfaces: Kinetics and Mechanisms" (2003). *Chemical and Biomolecular Engineering Faculty Research*. 16.
http://ideaexchange.uakron.edu/chemengin_ideas/16

This Article is brought to you for free and open access by Chemical and Biomolecular Engineering Department at IdeaExchange@UAkron, the institutional repository of The University of Akron in Akron, Ohio, USA. It has been accepted for inclusion in Chemical and Biomolecular Engineering Faculty Research by an authorized administrator of IdeaExchange@UAkron. For more information, please contact mjon@uakron.edu, uapress@uakron.edu.

Nanoscale oxidation of zirconium surfaces: Kinetics and mechanisms

N. Farkas
Department of Physics and Department of Chemistry, The University of Akron, Akron, Ohio 44325

G. Zhang and E. A. Evans
Department of Chemical Engineering, The University of Akron, Akron, Ohio 44325

R. D. Ramsier[a)]
Department of Physics, Department of Chemistry, and Department of Chemical Engineering, The University of Akron, Akron, Ohio 44325

J. A. Dagata
Precision Engineering Division, National Institute of Standards and Technology, Gaithersburg, Maryland 20899-8212

(Received 7 October 2002; accepted 23 December 2002; published 1 July 2003)

We show that atomic force microscope-induced oxide features can be formed reproducibly on both Zr and ZrN surfaces, and that the growth rate decreases rapidly with increasing time. There is an increase in oxide-feature height with humidity for both systems, and an approximately linear dependence of the height of the structures on the applied voltage for all films for short exposure times. As the anodization time increases, only the thinnest (6 nm) films show a large enhancement in oxide-feature height, demonstrating the role of the film/substrate interface. Under the same conditions, the height of features grown on ZrN films is greater than for those grown on Zr films, indicating that nitrogen plays a role in the oxidation process. © *2003 American Vacuum Society.* [DOI: 10.1116/1.1560712]

I. INTRODUCTION

Understanding surface reactions is critical to controlling the performance of engineering materials, and determining oxidation kinetics and growth mechanisms plays a major role in this effort. The corrosion resistant behavior of the zirconium materials system in nuclear and chemical applications is well known, and is normally attributed to the presence of a passivating oxide layer on the exposed surfaces. The growth of this layer, its modification with species such as nitrogen, and its resulting environmental stability are of importance for both corrosion mitigation and the development of thin nitride[1] and oxide[2] films for dielectrics. For these reasons, we have recently been studying the surface chemistry of hydrogen-, oxygen-, and nitrogen-containing species on single crystal Zr surfaces.[3–7]

Our previous results exhibit common phenomena associated with the high solid solubility of light atoms in Zr and rapid surface-subsurface diffusion kinetics. The subsurface region acts as a source or sink of reactants H, N, and O, depending on the conditions that in turn strongly influence the resulting thermal behavior of the surface. The rich and complex thermal kinetics that we observe for zirconium surfaces in vacuum have led us to study their electron-induced surface chemistry as well.[8,9] In particular, we have observed that low energy electron bombardment of adsorbed water and ammonia modifies the thermal desorption of hydrogen, and in the case of water leads to the formation of a partially oxidized surface following mild annealing.

These traditional surface-science studies are intrinsically connected to the work presented here, where we present a study of the growth of nanometer-scale oxide structures on Zr and ZrN surfaces using the atomic force microscope (AFM). (Disclaimer: Certain commercial equipment is identified in this article in order to describe the experimental procedure adequately. Such description does not imply recommendation or endorsement by NIST, nor does it imply that the equipment identified is necessarily the best available for the purpose.) AFM-induced local oxide patterning,[10–16] previously developed for nanolithography, is employed here as a means of investigating oxidation mechanisms on sputter-deposited Zr and ZrN thin films. Specifically, we examine the role of film thickness and nitrogen content in altering local oxide growth kinetics. In recent years, a considerable body of work has been published on the kinetics and mechanisms of AFM oxidation of metals, semiconductors, and insulators. Many aspects observed in these diverse materials systems are similar since the overall processes of ion transport and near-surface oxidation reactions driven by an extremely high electric field are often only slightly affected by specific reaction rates or ion mobilities. AFM oxidation allows us to access new energy and concentration regimes of the H, N, and O species present in the Zr system as compared to those studied by thermal or electron-beam techniques. Furthermore, these studies enable comparisons of Zr/ZrN behavior with results from AFM oxidation already available for other systems, such as Si/Si_3N_4 and Ti/TiN, in order to reveal some of the unique aspects of the zirconium materials system.

II. EXPERIMENT

Our experimental effort includes deposition of the thin Zr and ZrN films and AFM-induced local oxidation, followed

a)Author to whom correspondence should be addressed; electronic mail: rex@uakron.edu

Redistribution subject to AVS license or copyright; see http://scitation.aip.org/termsconditions. Download to IP: 130.101.140.126 On: Tue, 01 Apr 2014 00:21:38

TABLE I. Average and root-mean-square surface roughness of the films used in this work.

	Film thickness (nm)	Average roughness (nm)	Root-mean-square roughness (nm)
Zr	6	0.21	0.28
Zr/SiO_2	6	0.20	0.26
Zr	15	0.22	0.29
Zr	36	0.20	0.25
Zr+ZrN	36+2	0.27	0.34
Zr+ZrN	36+20	0.24	0.32

by characterization of the oxide structures. To prepare the thin films, Si(100) wafers are cut into 1 cm^2 pieces and serve as substrates. These are placed into a physical vapor deposition (PVD) chamber on a substrate holder located 8 cm above a Zr sputtering target. The substrate holder is grounded and the substrate temperature is not controlled during the deposition. The purity of the Zr target is 99.2% (Target Materials Inc.) including up to 4% Hf which occurs naturally with Zr ore. Major impurities are Fe (<1000 ppm), Cr (<4000 ppm), O (<1400 ppm), and C (<100 ppm). The turbomolecular-pumped vacuum system used in the deposition operates at a base pressure of 2.7×10^{-4} Pa. Radio frequency (rf) magnetron sputtering in a background of argon at 4.1–4.7 Pa is used to deposit the films. The deposition rate under these conditions with about 30 W of rf power is 0.02–0.05 nm/s as measured by a quartz crystal microbalance. Nitrogen is introduced into the PVD chamber to deposit ZrN. At the same pressures and powers as above, the ZrN deposition rate varies from 0.03 to 0.04 nm/s.

Using this standard PVD process, we prepare thinner (6 nm) and thicker (36 nm) Zr films on Si to investigate the effect of film thickness on AFM oxidation. Also, six nanometer films are deposited on clean Si substrates and wafers capped by a thermal SiO_2 barrier layer in order to investigate the role of Zr–Si interface reactions. Finally, in an attempt to alter the relevant chemistry and kinetics, 2 and 20 nm thick ZrN layers are sputter deposited on top of 36 nm Zr films before AFM oxidization.

AFM oxidation is performed under controlled ambient conditions in the laboratories at the National Institute for Standards and Technology (NIST) using a TopoMetrix Accurex II instrument in contact mode with W_2C-coated silicon cantilevers (Silicon-MDT Ltd.) as probes. To diminish tip-wear in contact mode, dots are formed on the surfaces and imaging is performed using a intermittent contact mode in most cases. The exposure times vary from 1 to 300 s and the dc bias voltages range from 5 to 15 V, with exposure parameters and tip positioning completely computer controlled. The relative humidity is in the range 21%–81% and is manipulated using a humidity-controlled glove box. The resulting oxide features are imaged using AFM with the same tips used for oxidation.

III. RESULTS AND DISCUSSION

A. Overview of the AFM oxidation process

During AFM oxidation the surface is positively biased with respect to the AFM tip, so the experimental parameters are the applied voltage, V, and the pulse duration time, t. Under ambient conditions the intense electric field at the tip–substrate junction causes a water meniscus to form, electrolysis of water molecules, and field-assisted transport of oxyanions into the substrate during the local anodic process. Transport of positively charged substrate ions may also occur, in accordance with classical anodic oxidation theory.[17,18] Thus localized surface reactions take place in the presence of hyperthermal (ionic and radical) species and may be influenced by local thermal effects due to Joule heating near the AFM tip. The most important advantage of using an AFM for this localized electrochemistry is that large-scale two-dimensional arrays of nanometer-scale oxide features which map the (V,t) parameter space can be produced on metallic, semiconducting, and insulating films.

B. Observations from the Zr/ZrN systems

Thin-film properties, particularly surface roughness and nanoscale homogeneity, play a determining role in minimizing feature size and maximizing reproducibility, both of which are essential requirements for studying local oxidation kinetics and understanding growth mechanisms. After sputtering, a native oxide layer starts to grow on our surfaces as soon as the films are exposed to air. In order to ensure that the surface has stabilized, AFM oxidation is carried out several days after the Zr films have been removed from the sputtering chamber. By this time the native oxide is a few nanometers thick and growing relatively slowly. AFM images (1×1 μm^2 in size) are recorded to determine the average and root-mean-square surface roughness of each Zr and ZrN film. Surface roughness values, between 0.2 and 0.4 nm, obtained for the samples used in this work are presented in Table I. The average standard deviation in these values is approximately 0.02 nm. The height of AFM oxide structures is typically just a few nanometers, therefore it is essential that the intrinsic surface roughness of the Zr and ZrN films be less than a nanometer.

As an example of the structures grown, Fig. 1 shows a representative AFM image of a sequence of oxide dots formed on a 20 nm thick ZrN film with exposure conditions of 8 V for 1–300 s at 21% relative humidity. Arrays of these features have been grown on all of our Zr and ZrN surfaces under various voltage, time, and humidity conditions, with excellent reproducibility. The dots are consistently symmetrical and well-defined in shape, indicating that tip wear is minimal since the imaging is done with the same tip used for oxidation. Using a stationary tip to draw dots rather than rastering to draw lines helps to minimize tip damage significantly, and will help us to understand the growth kinetics in the absence of scan-velocity-dependent hydrodynamic processes present with a rastering tip. Since our images of the oxide features are symmetric and of high quality, we feel that

Redistribution subject to AVS license or copyright; see http://scitation.aip.org/termsconditions. Download to IP: 130.101.140.126 On: Tue, 01 Apr 2014 00:21:38

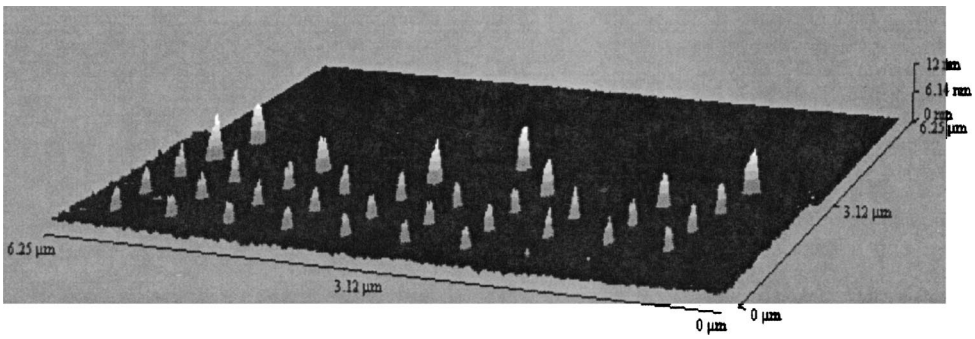

FIG. 1. AFM image of the oxide features produced on a 36 nm thick Zr film with a 20 nm thick ZrN capping layer using 8 V for 1–300 s at 21% relative humidity.

potential material transfer to the tip during oxidation or imaging is not a major factor in this study.

Focusing first on time dependence, Fig. 2 demonstrates that both the vertical and lateral growth rates of the oxides formed on Zr and ZrN films with an AFM decrease rapidly with increasing time. Power-law relationships of height versus AFM anodization time are also found for AFM oxidation of Ti,[19,20] TiN,[21] Si,[12–16] and Si_3N_4 surfaces.[22–24] This type of power-law behavior is due in part to the space charge built up in the early period of local oxidation using dc voltages.[25–33] Space charge is a consequence of unbalanced ionic reactants and products, mainly O- and H-containing species, generated during oxidation. This in turn leads to oxides with a lower density than expected.

We also find that the height of the oxide features for the Zr and ZrN systems increases linearly with humidity at long anodization times ($t>200$ s), which is also observed for the anodic oxidation of Ti films.[19,20,30] For a given tip–surface distance and AFM tip geometry, the equilibrium shape of the meniscus depends on the humidity and the applied voltage. Since the local reaction volume is defined by the meniscus, it is important to distinguish material-dependent factors that contribute to the growth rate from those depending solely on the meniscus. To demonstrate this distinction, we take the long-time height and width data of Fig. 2 and re-plot these in Fig. 3 versus relative humidity. Clearly, material dependence can be observed in the height data in the top of Fig. 3, whereas the bottom of Fig. 3 demonstrates that the width data are independent of film composition or thickness. Different substrate compositions may lead to variations in wetting behavior, changing the equilibrium contact angle of the meniscus with the surface and therefore its shape. Since the meniscus is a dielectric medium through which the electric field propagates, changes in the shape of the meniscus could result in a different electric field distribution and thus variations in the width of the oxide features with materials system. The bottom panel of Fig. 3 suggests that this effect is not dominant in the work we are reporting here. In this study we find that AFM oxide patterning is not reproducible at less than 20% relative humidity, as noted by other researchers.[34]

Although the overall behavior of the growth curve is similar for Zr and ZrN, we see in Fig. 3 that the height of the features grown on ZrN films is consistently greater than those on Zr films, roughly by a factor of 2. Previous work with nitrogen-containing species on single crystal zirconium indicates that nitrogen atoms can readily displace subsurface oxygen, known to be intrinsic to crystalline zirconium, effectively forcing oxygen to the surface where it combines with hydrogen during thermal desorption experiments to form water.[3–5,8] This desorption of water is accompanied by ammonia as well, but disproportionately leaves strongly bound residual nitrogen behind at the surface. We believe that this

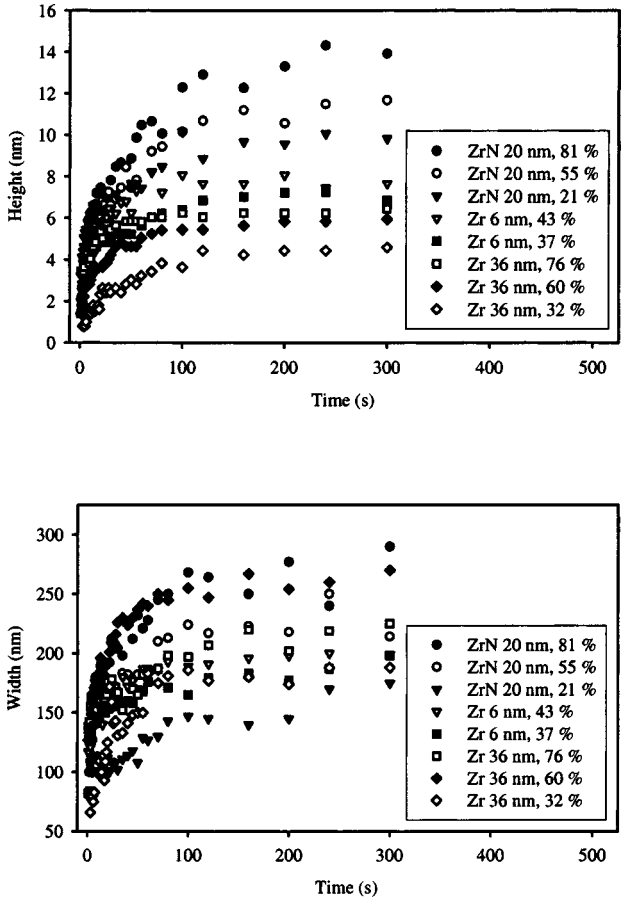

FIG. 2. Time dependence of the oxide-feature height (top) and width (bottom) on Zr and ZrN films. The applied voltage is 8 V and relative humidity varies from 21% to 81%. The legend also indicates the film thickness in each case.

Redistribution subject to AVS license or copyright; see http://scitation.aip.org/termsconditions. Download to IP: 130.101.140.126 On: Tue, 01 Apr 2014 00:21:38

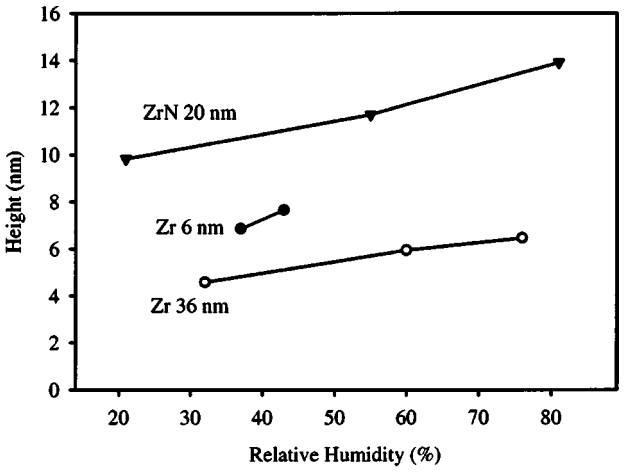

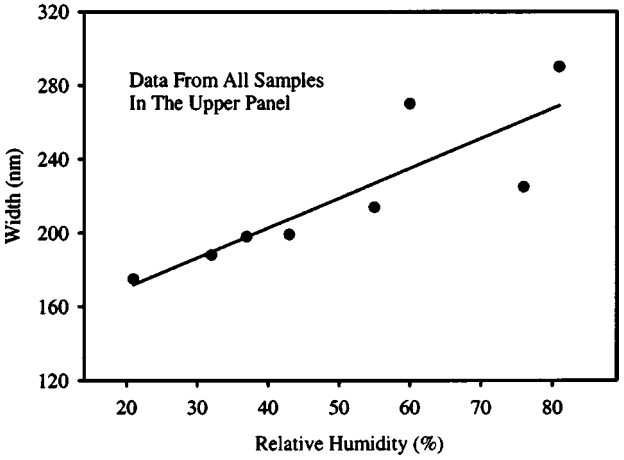

FIG. 3. Height and width vs humidity data for Zr and ZrN films replotted from Fig. 2. Clearly the width of AFM oxide features exhibits no material dependence and is simply a function of humidity. On the other hand, the height is sensitive to film composition and thickness.

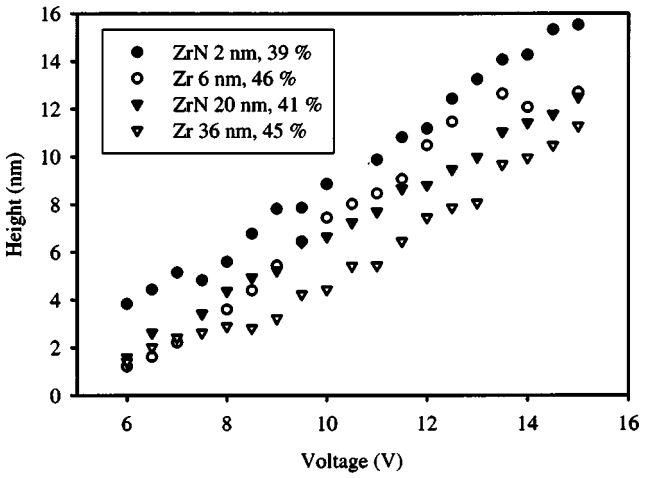

FIG. 4. Voltage dependence of the oxide-feature heights on Zr and ZrN films. The exposure time is 5 s. The legend also indicates the film thickness in each case.

displacement and water-formation reaction is in some sense the reverse reaction of what we are reporting here, where oxyanions, driven by an applied electric field, oxidize the zirconium nitride surface.

Our interpretation is that the presence of nitrogen, even in a relatively strongly bound state, enhances the oxidation of zirconium films because it is able to react efficiently with hydrogen and leave the system as a by-product. Evidence for this conjecture is based on our previous electric potential imaging of oxide structures produced on silicon with an AFM that demonstrates positive charge buildup during oxidation and doping-dependent differences.[25,26] We attribute this effect to H^+ ions liberated from hydroxyl species during oxide growth at the silicon–oxide interface. Additional work by Marchi *et al.*,[15] using UV/ozone in place of water, confirms that in the absence of hydrogen ions the differences expected based on hole concentration arguments between *n*- and *p*-type silicon are obtained. Furthermore, Gwo *et al.*[22–24] also report a significant enhancement in the oxidation kinetics of Si_3N_4 films relative to silicon. Using Auger microprobe and synchrotron photoemission, they demonstrate convincingly that areas locally oxidized by AFM are completely depleted of nitrogen.[24] We do not presently have chemical analysis data from our nanoscale structures on Zr and ZrN surfaces to accurately pinpoint the fate of H and N species.

AFM oxidation of titanium and titanium nitride thin films provides a contrast to the behavior of the Zr and ZrN system. Gwo *et al.*[21] also report studies of TiN oxidation kinetics that indicate nitridation leads to slower, rather than faster, oxide growth. This difference may be due to a combination of at least three factors. First of all, although the optical constants of both ZrN and TiN indicate free-electron behavior for both films,[35,36] subsurface nitrogen may be less strongly bound and more mobile in ZrN than in TiN films. In addition, the oxygen bond energy is greater by roughly 100 kJ/mol for Zr than it is for Ti.[37] Finally, the solid solubility in the near-surface layer of Zr films may be greater than in Ti thin films. This line of reasoning is consistent with a growing body of evidence from kinetic studies of aluminum films that suggest positive ion transport can play an important role in AFM oxidation, especially for very thin films on highly insulating substrates.[38]

Turning now to an investigation of voltage-dependent behavior for Zr and ZrN films, Fig. 4 indicates an approximately linear dependence between the height of the oxide structures grown with an AFM and the applied voltage for all films in the case of short exposure times, i.e., when the exposure time is 5 s or less. Note that this corresponds to exposure times before the significant change in slope in the plots of Fig. 2. This behavior is a general characteristic of the AFM-induced anodization process and a similar voltage dependence has been reported for a variety of materials systems.[12–16,19–33] In our case there is an apparent minimum threshold voltage of 5 V for the growth to initiate which may reflect the resistive or dielectric aspects of the native oxide present on the Zr and ZrN thin films.

It is important to recognize the connection between AFM oxidation experiments, which easily access high electric-field

Redistribution subject to AVS license or copyright; see http://scitation.aip.org/termsconditions. Download to IP: 130.101.140.126 On: Tue, 01 Apr 2014 00:21:38

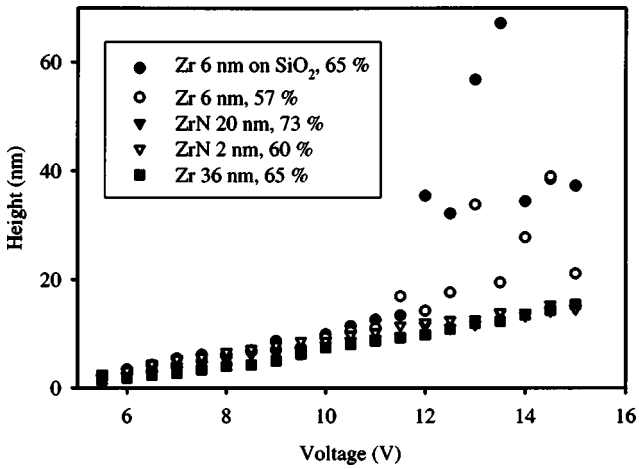

FIG. 5. Voltage dependence of the oxide-feature heights on Zr and ZrN films. The exposure time is 20 s. The legend also indicates the film thickness in each case.

driven growth conditions, and the models developed years ago in the theoretical anodic oxidation literature.[17,18] Essentially all of these models incorporate high-field approximations for anodic surface oxidation processes in order to make calculations tractable. However, the electric fields in normal anodization mechanisms are not easily varied nor are these fields of the genuine high-field limit, since they represent a process internal to the system. In contrast, we have external control over the local field, covering an enormous range, through the applied voltage. By systematically varying the composition of metallic thin films, such as aluminum, titanium, niobium, etc., we can begin to relate the classical models to specific materials systems. Different systems provide variations in metal ion solubility in the growing oxide film, metal reactivity with oxyanions, oxide stability and structure, and the presence of nitrogen which opens up alternative reaction pathways.

Figure 5 demonstrates that the thin 6 nm Zr/Si and 6 nm Zr/SiO_2 films exhibit nonmonotonic increases in oxide-feature height after a certain voltage is reached when the exposure time is 20 s, whereas the linear behavior of the other systems is unchanged. This behavior is in marked contrast to what is observed on thin films of Ti (Ref. 39) and Al (Ref. 38) in which an overall attenuation of the growth curve occurs as the film becomes thinner. In the work reported here, the jump in the growth kinetics only appears above a certain voltage for very thin Zr films.

Comparing the short (5 s) and long (20 s) exposure kinetics is therefore a means through which we can understand the role of the interface with the substrate. If this nonlinear behavior occurred near the same voltage independent of exposure time, we might rationalize some type of dielectric breakdown in the system, perhaps of the native oxide film. However, the resulting oxide features do not resemble typical breakdown events, since the well-formed shape of our structures exhibits a greater height without an appreciable increase in width. In addition, breakdown usually produces irregular cratering of the surface, not the smooth mounds that we observe. Since it only occurs for the thinnest films at the longest times, we must consider that the oxide features advance into the film as well as rise above it as they grow. When this advancing front reaches the film/substrate interface the chemical kinetics change, causing a jump in the oxide feature height. This may be due to an increased rate of transport of metal ions or even Si substrate atoms into the reaction zone, perhaps by lateral diffusion along the substrate/film interface. Such lateral diffusion is probably due to distortion of the electric field as the moving oxide–metal boundary approaches the insulating substrate. In fact, this must be the case for films only a few nanometers thick in order to account for the dependence of the overall oxide growth rate on film thickness.[39] Field distortion is even capable of enhancing, rather than suppressing, oxide growth near dielectric edges of very thin Al films.[38] Without stoichiometric data on the nanoscale features, we cannot do more than hypothesize at present regarding this nonlinear behavior.

C. Relationship of present results to existing models and data

As we progress toward more comprehensive models of AFM-induced oxidation,[25–33] we find not only observations common to many materials systems but also system-specific behavior. It is known that Ti films can be oxidized using scanning probe techniques,[19,20,30] and our use of chemically similar Zr allows us to compare which surface chemical properties of the substrate are most important for nanolithography of metals. We see that humidity is important as expected,[14,16,31] with an increase in feature height with humidity for all Zr and ZrN surfaces studied. We also find that very small surface roughness and good control over the applied voltage sequence is critical for reproducible results, as our initial attempts to study growth kinetics on lower-quality Zr surfaces without a computer-controlled voltage source proved unsuccessful.

Our results for AFM-induced oxide growth on Zr and ZrN surfaces show kinetics similar to those seen in other metal and semiconductor systems, with generally similar feature dimensions and time/voltage characteristics. This would seem to indicate that the major factors influencing the growth are inherent to the method itself, and not to the details of the surface chemistry. This strengthens arguments that the AFM-based technique is transferable across materials systems, which greatly enhances its potential role in nanofabrication technology. However, it also leads to fundamental questions as to why the results are somewhat insensitive to the surface chemistry which we know strongly depends on the material system in other contexts. The answer to these questions may lie in the presence of very high electric fields and a resulting dominance by hyperthermally driven surface reactions involving ionic and radical species during AFM oxidation. Such species are not present during standard surface kinetic studies, and their concentration and flux at the surface even in normal electrochemical measurements is certainly much lower than in the nanolithography process.

Redistribution subject to AVS license or copyright; see http://scitation.aip.org/termsconditions. Download to IP: 130.101.140.126 On: Tue, 01 Apr 2014 00:21:38

IV. CONCLUSIONS

We demonstrate the local oxidation of Zr and ZrN thin-film surfaces using AFM lithographic techniques. We find that the growth of nanoscale features, both vertically and laterally, exhibits rapid kinetics initially followed by a crossover to slower processes. The size of the features increases with applied voltage and humidity, and the presence of nitrogen in the films enhances the growth. For longer exposure times and higher voltages, the thinnest films exhibit nonlinear behavior attributed to the involvement of the film–substrate interface.

ACKNOWLEDGMENTS

Acknowledgment is made to the Donors of the American Chemical Society Petroleum Research Fund for partial support of this research. Partial support from Research Corporation is also acknowledged. Support from the NIST Office of Microelectronics Programs is also acknowledged.

[1]L. Pichon, A. Straboni, T. Girardeau, M. Drouet, and P. Widmayer, J. Appl. Phys. **87**, 925 (2000).
[2]S. Ramanathan, C.-M. Park, and P. C. McIntyre, J. Appl. Phys. **91**, 4521 (2002).
[3]Y. C. Kang, D. A. Clauss, and R. D. Ramsier, J. Vac. Sci. Technol. A **19**, 1996 (2001).
[4]Y. C. Kang and R. D. Ramsier, Vacuum **64**, 113 (2002).
[5]Y. C. Kang and R. D. Ramsier, J. Nucl. Mater. **303**, 125 (2002).
[6]Y. C. Kang and R. D. Ramsier, Appl. Surf. Sci. **195**, 196 (2002).
[7]Y. C. Kang and R. D. Ramsier, Surf. Sci. **519**, 229 (2002).
[8]N. Stojilovic, Y. C. Kang, and R. D. Ramsier, Surf. Interface Anal. **33**, 945 (2002).
[9]S. Ankrah, Y. C. Kang, and R. D. Ramsier (unpublished).
[10]J. A. Dagata, J. Schnier, H. H. Harary, C. J. Evans, M. T. Postek, and J. Bennett, Appl. Phys. Lett. **56**, 2001 (1990).
[11]E. S. Snow and P. M. Campbell, Appl. Phys. Lett. **64**, 1932 (1994).
[12]T. Teuschler, K. Mahr, S. Miyasaki, M. Hundhausen, and L. Ley, Appl. Phys. Lett. **67**, 3144 (1995).
[13]D. Stievenard, P. A. Fontaine, and E. Dubois, Appl. Phys. Lett. **70**, 3272 (1997).
[14]P. Avouris, T. Hertel, and R. Martel, Appl. Phys. Lett. **71**, 285 (1997).
[15]F. Marchi, V. Bouchiat, H. Dallaporta, V. Safarov, D. Tonneau, and P. Doppelt, J. Vac. Sci. Technol. B **16**, 2952 (1998).
[16]R. García, M. Calleja, and F. Pérez-Murano, Appl. Phys. Lett. **72**, 2295 (1998).
[17]M. J. Dignam, in *Oxides and Oxide Films*, edited by J. W. Diggle (Marcel Dekker, New York, 1972), Vol. 1, p. 92.
[18]A. T. Fromhold, in *Oxides and Oxide Films*, edited by J. W. Diggle and A. K. Vijh (Marcel Dekker, New York, 1976), Vol. 3, p. 1.
[19]R. Held, T. Heinzel, P. Studerus, and K. Ensslin, Physica E (Amsterdam) **2**, 748 (1998).
[20]R. V. Vullers, M. Ahlskog, M. Cannaerts, and C. Van Haesendonck, J. Vac. Sci. Technol. B **17**, 2417 (1999).
[21]S. Gwo, C.-L. Yeh, P.-F. Chen, Y.-C. Chou, T. T. Chen, T.-S. Chao, S.-F. Hu, and T.-Y. Huang, Appl. Phys. Lett. **74**, 1090 (1999).
[22]F. S.-S. Chien, J.-W. Chang, S.-W. Lin, Y.-C. Chou, T. T. Chen, S. Gwo, T.-S. Chao, and W.-F. Hsieh, Appl. Phys. Lett. **76**, 360 (2000).
[23]F. S.-S. Chien, Y. C. Chou, T. T. Chen, W.-F. Hsieh, T.-S. Chao, and S. Gwo, J. Appl. Phys. **89**, 2465 (2001).
[24]R. Klauser, I.-H. Hong, H.-J. Su, T. T. Chen, S. Gwo, S.-C. Wang, T. J. Chuang, and V. A. Gritsenko, Appl. Phys. Lett. **79**, 3143 (2001).
[25]J. A. Dagata, T. Inoue, J. Itoh, and H. Yokoyama, Appl. Phys. Lett. **73**, 271 (1998).
[26]J. A. Dagata, T. Inoue, J. Itoh, K. Matsumoto, and H. Yokoyama, J. Appl. Phys. **84**, 6891 (1998).
[27]J. A. Dagata, F. Perez-Murano, G. Abadal, K. Morimoto, T. Inoue, J. Itoh, and H. Yokoyama, Appl. Phys. Lett. **76**, 2710 (2000).
[28]K. Morimoto, F. Pérez-Murano, and J. A. Dagata, Appl. Surf. Sci. **158**, 205 (2000).
[29]A. Avramescu, A. Ueta, K. Uesugi, and I. Suemune, J. Appl. Phys. **88**, 3158 (2000).
[30]E. Dubois and J.-L. Bubendorff, J. Appl. Phys. **87**, 8148 (2000).
[31]H. Bloeß, G. Staikov, and J. W. Schultze, Electrochim. Acta **47**, 335 (2001).
[32]S. Lemeshko, S. Gavrilov, V. Shevyakov, V. Roschin, and R. Solomatenko, Nanotechnology **12**, 273 (2001).
[33]D. V. Sokolov, Tech. Phys. **47**, 58 (2002).
[34]R. Garcia and F. Perez-Murano (private communication).
[35]M. Veszelei, K. Andersson, C.-G. Ribbing, K. Jarrendahl, and H. Arwin, Appl. Opt. **33**, 1993 (1994).
[36]R. M. Costescu, M. A. Wall, and D. G. Cahill, http://users.mrl.uiuc.edu/cahill/condepi.pdf
[37]*CRC Handbook of Chemistry and Physics*, 69th ed., edited by R. C. Weast (CRC, Boca Raton, FL, 1988), p. F177.
[38]J. A. Dagata and F. Perez-Murano (unpublished).
[39]Figures 2 and 3 of Ref. 32.

Redistribution subject to AVS license or copyright; see http://scitation.aip.org/termsconditions. Download to IP: 130.101.140.126 On: Tue, 01 Apr 2014 00:21:38